Universality in nonadiabatic behavior of classical actions in nonlinear models of Bose-Einstein condensates

A. P. Itin[1,2] and S. Watanabe[1]

[1]*Department of Applied Physics and Chemistry, University of Electro-Communications, 1-5-1, Chofu-ga-oka, Chofu-shi, Tokyo 182-8585, Japan*

[2]*Space Research Institute, Russian Academy of Sciences, Profsoyuznaya str. 84/32, 117997 Moscow, Russia*

(Received 6 November 2006; published 28 August 2007)

We discuss the dynamics of approximate adiabatic invariants in several nonlinear models being related to the physics of Bose-Einstein condensates (BECs). We show that the nonadiabatic dynamics in Feshbach resonance passage, nonlinear Landau-Zener (NLZ) tunneling, and BEC tunneling oscillations in a double well can be considered within a unifying approach based on the theory of separatrix crossings. The separatrix crossing theory was applied previously to some problems of classical mechanics, plasma physics, and hydrodynamics, but has not been used in the rapidly growing BEC-related field yet. We derive explicit formulas for the change in the action in several models. Extensive numerical calculations support the theory and demonstrate its universal character. We also discovered a nonlinear phenomenon in the NLZ model which we propose to call *separated adiabatic tunneling*.

DOI: 10.1103/PhysRevE.76.026218 PACS number(s): 32.80.Pj, 03.65.−w

I. INTRODUCTION

Adiabatic invariance [1] is very important in many fields of physics. In the last decade, there has been a great deal of interest in the physics of Bose-Einstein condensates (BECs) [2–7] among scientists from several scientific fields. Presently BEC research is at the crossing point of atomic, molecular, and optical (AMO) science, statistical mechanics and condensed matter physics, nonlinear dynamics, and chaos. The discussion we present here is related to the interplay between nonlinearity and nonadiabaticity in BEC systems. The relation between quantum transitions and change in the classical action of a harmonic oscillator has long been known [8,9]. BECs bring nonlinearity into a quantum world. BEC dynamics can often be described within the mean-field approximation; finite-mode expansions produce nonlinear models where a variety of phenomena common to classical nonlinear systems happen. We consider two kinds of nonlinear phenomena here: destruction of adiabatic invariance at separatrix crossings and probabilistic captures in different domains of phase space.

A conceptual phenomenon of classical adiabatic theory is the destruction of adiabatic invariance at separatrix crossings which is encountered, in particular, in plasma physics and hydrodynamics and classical and celestial mechanics [10–22]. The phenomenon is very important for BEC physics: we consider here nonlinear two-mode models related to tunneling between coupled BECs in a double well [23], nonlinear Landau-Zener tunneling [24,25], and Feshbach resonance passage in atom-molecule systems [26–28]. Nonlinear two-mode models were extensively studied previously (sometimes beyond the mean-field approximation [23–25,29–44]), and destruction of adiabaticity was discussed already in [24–26]; still, there are regimes of motion that were not analyzed in these papers from the point of view of nonadiabatic behavior—that is, when initial populations of both modes are not zero (or very small), but finite. We presented some of our results on that theme in [27,28]; nevertheless, destruction of adiabatic invariance has not been studied systematically in BEC-related models yet. The action is an approximate adiabatic invariant in a classical Hamiltonian system that depends on a slowly varying parameter provided a phase trajectory stays away from separatrices of the unperturbed (frozen at a certain parameter value) system. If this condition is not met, adiabaticity may be destroyed. As the parameter varies, the separatrices slowly evolve on the phase portrait. A phase trajectory of the exact system may come close to the separatrix and cross it. The general theory of the adiabatic separatrix crossings [10] predicts universal behavior of the classical action (described in a greater detail in the main text). In particular, at the separatrix crossing the action undergoes a quasirandom *dynamical* jump, which is very sensitive to initial conditions and depends on the rate of change of the parameter. The asymptotic formula for this jump was obtained in [11–13]. Later, the general theory of adiabatic separatrix crossings was also developed for slow-fast Hamiltonian systems [10,17] and was applied to certain physical problems (see, for example, [16,18–20]). It was also noticed that nonlinear Landau-Zener (NLZ) tunneling models constitute a particular case for which the general theory can be applied [27,28]. Beside the quasirandom jumps of adiabatic invariants, there is another important mechanism of stochastization in BEC-related models: scattering on an unstable fixed point with a capture into different regions of phase space after a separatrix crossing [45–47]. Here stochastization happens due to quasirandom splitting of phase flow in different regions of phase space at the crossing. A rigorous definition of such probabilistic phenomena in dynamical systems was given in [48]. The probabilistic capture is important in problems of celestial mechanics [10], but it was also investigated in some problems of plasma physics and hydrodynamics [16], optics [18], classical billiards with slowly changing parameters, and other classical models [19]. As shown in [47], the combination of the two phenomena leads to a *dephasing* in the dynamics of globally coupled oscillators modeling coupled Josephson junctions. However,

it seems that the probabilistic capture mechanism was not discussed at all in relation to BEC models yet. We discovered that in a nonlinear Landau-Zener model such a mechanism may take place, and it leads to a new phenomenon (in the context of the model) which we propose to call *separated adiabatic tunneling*.

Let us review the models being considered in the present paper in more concrete terms. The nonlinear two-mode model introduced in [23] describes BEC tunneling oscillations in a double well as that of a nonrigid pendulum. In the case of an asymmetric double well, the effective classical Hamiltonian is

$$H = -\delta w + \frac{\lambda w^2}{2} - \sqrt{1-w^2}\cos\theta, \tag{1}$$

where w and θ are the population imbalance and phase difference between the two modes and the parameters δ and λ represent the potential difference between the wells and nonlinearity, correspondingly. The same Hamiltonian appears in a nonlinear Landau-Zener model [24,25]. As one slowly sweeps δ, say, from a large positive to a large negative value, a change in the mode populations is determined by the change in the classical action (since at large $|\delta|$ classical action depends linearly on w). This provides an interesting link between the fundamental issue of classical mechanics, dynamics of approximate adiabatic invariants (classical actions), and nonadiabatic transitions in quantum many-body systems. The dynamics of classical actions in nonlinear systems is, however, a very complicated issue [10]. Some analysis of the NLZ model was done in [24,25]. In [25] so-called subcritical ($\lambda<1$), critical ($\lambda=1$), and supercritical ($\lambda>1$) cases were defined. However, only the case of zero initial action was considered—that is, a vanishingly small initial population in one of the states. We concentrate on the case of finite initial action and supercritical case. In the supercritical case, the most striking phenomenon from the point of view of physics is the so-called *nonzero adiabatic tunneling* (nonzero AT). In terms of the theory of separatrix crossings, it is caused by the *geometric* jump in the action at the separatrix crossing. Mathematically, it is a very simple issue: as a phase point leaves a domain bounded by a separatrix of the unperturbed system and enters another domain, its action undergoes a "geometric" change proportional to the difference in areas of the two domains [49]. The gist of *separated adiabatic tunneling* (separated AT) that we found is as follows. The separatrix divides the phase portrait into three domains $G_{1,2,3}$ (Fig. 9). In case at the moment of the separatrix crossing the areas of $G_{1,2}$ grow, the phase point leaving the third domain G_3 (with decreasing area) can be captured in either of the two growing domains. A bunch of trajectories with close initial actions I_i will be "split" into two bunches with two different final actions $I_f^{1,2}$. It is possible to calculate the probability for a phase point to come to either of the two bunches (we calculated it in Appendix B and compared the analytical prediction with the numerical result in Fig. 11). The possible physical applications of the nonzero AT phenomenon have been extensively discussed (for example, [24,25]: the wave packet in an accelerated optical lattice should undergo nonzero tunneling in the adiabatic limit when nonlinearity is large enough, although no experimental evidence is available yet). In relation to BEC oscillations in an asymmetric double well, the corresponding physical effect is a (obvious) drastic change in the amplitude of oscillations when the regime of motion is changed from self-trapped to complete oscillations due to a slow change of parameters. In the case of *separated AT*, the effect for the asymmetric double well may look like this: the asymmetry between the wells is slowly changed; the regime of motion is changed from self-trapped to complete oscillations and then back to self-trapped. But the final state is quasirandom: a system has the "choice" of two different final states. For a set of experimental realizations with close initial conditions, one can define the "probability" for a system to come to either of the two states. While such an experimental realization seems to be even less realistic than nonzero AT, conceptually it is a very interesting phenomenon worth discussing: the probability is of purely classical origin. An analogous interpretation can be done for BECs experiencing NLZ tunneling in the optical lattice. Although the phenomenon looks similar to the nonzero AT described in [24,25], its mathematical background is very much different and not so straightforward; it is a particular case of probabilistic phenomena in dynamical systems being defined in [48].

We also derive a formula for the jump of the adiabatic invariant [Eq. (23)] in the symmetric well case ($\delta=0$) and check it numerically (for the asymmetric case, the corresponding formula has both terms of order ϵ and $\epsilon\ln\epsilon$). As a physical application of this jump, one can imagine an experiment with BEC oscillations in a double well, with the potential barrier between the wells being slowly raised and then slowly decreased back to its initial position. The system will not return back to its initial state. Within the mean-field two-state model, the difference between the initial and final oscillations is caused by the change in the adiabatic invariant (of course, in a real system many other complications arise). Such kinds of experiments are feasible [50,51].

Similar nonadiabatic phenomena arise in coupled atom-molecular systems. Here, in the mean-field limit it is possible to construct two-mode models based on the all-atom and all-molecule modes and their coherent superpositions. [52,53] The two-mode model describing a degenerate gas of fermionic atoms coupled to bosonic molecules was considered in [26–28] (the same model enables us to describe coupled atomic and molecular BECs, so we call it the two-mode AMBEC model). The system is reduced to the classical Hamiltonian

$$H = -\delta(\tau)w + (1-w)\sqrt{1+w}\cos\theta, \tag{2}$$

where w denotes population imbalance between atomic and molecular modes and δ is the (slowly changing) detuning from the Feshbach resonance. As δ sweeps from large positive to negative values, the system is transferred from the all-atom $w=1$ mode to the all-molecule $w=-1$ mode. The final state of the system contains the nonzero atomic remnant fraction, which can be calculated as a change in the classical action in the model (2), and scales as a power law of the sweeping rate. The model was introduced in [26] in an at-

tempt to describe recent experiments on Feshbach resonance passage [54–57], and some power laws were calculated there and compared with experimental data. For the case of nonzero initial molecular fraction, the power law was also calculated in [27,28] according to the general theory. We carefully check numerically this (linear) power law in Sec. II B. It is important to note that the model gives 100% conversion efficiency in the adiabatic limit, while in the experiments finite conversion efficiency has been seen. In Sec. II C we present a brief analysis of a more general model, which has an analog of nonzero AT (leading to finite conversion efficiency in the adiabatic limit). In the more general version, *s*-wave interactions were taken into account, so the Hamiltonian looks like

$$H = -\delta w + \lambda w^2 + (1-w)\sqrt{1+w}\cos\theta. \tag{3}$$

Here, the phase portraits can have more complicated structure and the passage through the separatrix can be accompanied by the geometric jump in the action, leading to a nonzero remnant fraction even in the adiabatic limit.

In Sec. III, the nonlinear two-mode model (1) for two coupled BECs is considered. For brevity, we call this model the two-mode atomic BEC (ABEC) model. The separated AT is demonstrated in the end of the section.

Section IV contains concluding remarks. In Appendix A we described the adiabatic and improved adiabatic approximations. In Appendix B, a derivation of the formula for probabilities in separated AT is presented.

The most interesting new results of the paper are the following.

(i) Extensive numerical tests of the formula (12) for the dynamical jump in the adiabatic invariant of the atom-molecule system (Sec. II B). The formula is based on Eq. (10) which is obtained elsewhere [27,28].

(ii) Suggested mechanism (analog of nonzero AT, Sec. II C, Fig. 2) leading to finite conversion efficiency in atom-molecule systems due to a geometric jump in the action.

(iii) Analytical derivation of the explicit expression (23) for the jump of adiabatic invariant of the symmetric ABEC model and its numerical test (Sec. III B, Fig. 8).

(iv) Discovery of a phenomenon in the nonlinear Landau-Zener model: *separated AT*. Analytical calculation of probabilities related to this tunneling (B32-34) and its numerical test (Sec. III C, Fig. 11).

The *main* result is demonstration of the usefulness of separatrix crossing theory in a variety of BEC-related models. In order to keep the paper compact, we do not present here a comparison with quantum many-body calculations, but consider only mean-field models.

II. NONLINEAR TWO-MODE MODELS FOR ATOM-MOLECULAR SYSTEMS

A. Model equations and its physical origin: Classical phase portraits

In BEC-related mean-field models nonlinearity usually comes from *s*-wave interactions (via a scattering length entering the nonlinear term of the Gross-Pitaevskii equation [6]). However, interesting nonlinear models arise in atom-molecular systems, where atoms can be converted to BECs of molecules. Even neglecting collisions and corresponding *s*-wave interactions, the nonlinearity comes into play from the fact that two atoms are needed to form a molecule.

We consider a Hamiltonian system with the Hamiltonian function

$$H = -\delta(\tau)w + \lambda w^2 + (1-w)\sqrt{1+w}\cos\theta, \tag{4}$$

where $\tau=\epsilon t$, $\epsilon \ll 1$. Several systems can be described by the model (4), in particular coupled atomic and molecular BECs [35] and a gas of fermionic atoms coupled to molecular BECs [26–28]. Let us briefly discuss these systems.

In [35], a system of coupled atomic and molecular condensates was considered using a generalization of the Bloch representation for the two-mode system. The quantum Hamiltonian of the system is $\hat{H}=\frac{\Delta}{2}a^\dagger a+\frac{\Omega}{2}(a^\dagger a^\dagger b+b^\dagger aa)$, where $a^\dagger$ and a are the creation and annihilation operators of the atomic mode, while $b^\dagger$ and b are the creation and annihilation operators of the molecular mode. The two modes are supposed to be coupled by means of a near-resonant two-photon transition or a Feshbach resonance, with a coupling frequency Ω and detuning Δ. Introducing the operators $\hat{L}_x=\sqrt{2}\frac{a^\dagger a^\dagger b+b^\dagger aa}{N^{3/2}}$, $\hat{L}_y=\sqrt{2}\frac{a^\dagger a^\dagger b-b^\dagger aa}{iN^{3/2}}$, and $L_z=\frac{2b^\dagger b-a^\dagger a}{N}$, Heisenberg equations of motion in the mean-field limit lead to a dynamical system for the rescaled components of the generalized Bloch vector: $\dot{s}_x=-\delta s_y$, $\dot{s}_y=-\frac{\sqrt{2}}{4}(s_z-1)(3s_z+1)+\delta s_x$, and $\dot{s}_z=-\sqrt{2}s_y$, where the rescaled detuning is $\delta=\Delta/(\sqrt{N}\Omega)$, while $s_{x,y,z}$ are the expectation values of $L_{x,y,z}$ ($s_z=1$ corresponds to the all-molecule mode; N is the number of atoms). Exactly the same dynamical system arises in the degenerate model of fermionic atoms coupled to BECs of diatomic molecules [26]. Indeed, using a similar approach in [26] an analogous system of equations was obtained:

$$\dot{u} = \delta(\tau)v,$$

$$\dot{v} = -\delta(\tau)u + \frac{\sqrt{2}}{4}(w-1)(3w+1),$$

$$\dot{w} = \sqrt{2}v, \tag{5}$$

where w is the population imbalance between the all-atom and all-molecule modes, u and v are real and imaginary parts of the atom-molecule coherence, and δ is the rescaled detuning from the resonance. These equations are equivalent to the Hamiltonian equations of motion of the Hamiltonian system (4) with $\lambda=0$ [27]. The variable θ canonically conjugated to w is related to the old variables as $\theta=\arctan(v/u)$. The all-atom mode now corresponds to $w=1$, while the all-molecule mode to $w=-1$. Sweeping through Feshbach resonance from fermionic atoms to Bose molecules can be described by the Hamiltonian (4) with $\lambda=0$ and δ slowly changing from large positive to large negative values. In both systems (atom-molecule BECs and degenerate fermionic gas coupled to BECs of molecules) mean-field collisional interactions were neglected so far. The case $\lambda\neq 0$ in the Hamiltonian (4) corresponds to inclusion of the *s*-wave scattering interactions.

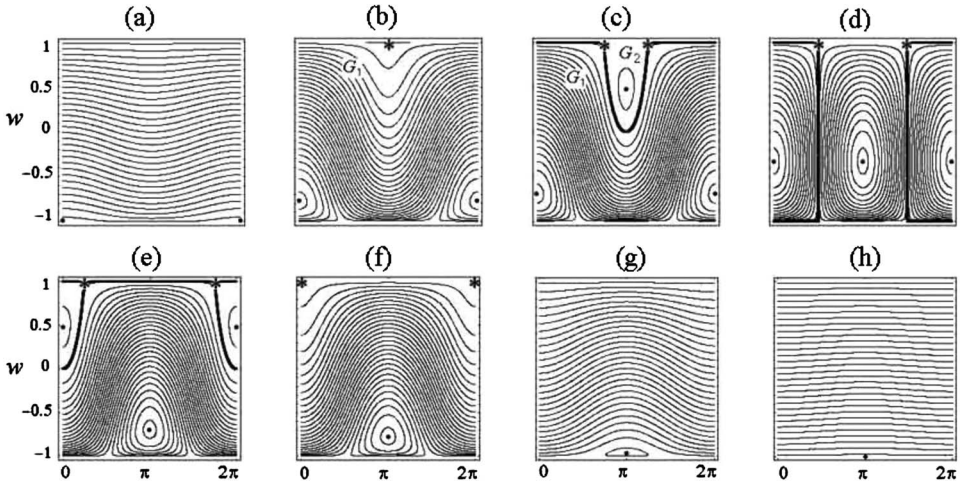

FIG. 1. Phase portraits of the Hamiltonian (4) with $\lambda=0$. From left to right: $\delta=10$, $\sqrt{2}$, 1, 0, −1, $-\sqrt{2}$, −5, −50. Stars (bold dots): unstable (stable) fixed points. See detailed discussion in [27,28]

Recently, in [43] a more general quantum Hamiltonian describing the coupling between atomic and diatomic-molecular BECs within two-mode approximation was considered:

$$H = U_a N_a^2 + U_b N_b^2 + U_{ab} N_a N_b + \mu_a N_a + \mu_b N_b + \Omega(a^\dagger a^\dagger b + b^\dagger a a), \tag{6}$$

where $a^\dagger$ is the creation operator for an atomic mode while $b^\dagger$ creates a molecular mode; parameters U_i describe S-wave scattering: atom-atom (U_a), atom-molecule (U_{ab}), and molecule-molecule (U_b). The parameters μ_i are external potentials, and Ω is the amplitude for the interconversions of atoms and molecules. N_a and N_b are populations of the atomic and molecular modes, correspondingly. In the limit of large $N=N_a+2N_b$, the classical Hamiltonian was obtained:

$$H = \lambda z^2 + 2\alpha z + \beta + 2\sqrt{1-z}(1+z)\cos(4\theta/N), \tag{7}$$

where

$$\lambda = \frac{\sqrt{2N}}{\Omega}(U_a/2 - U_{ab}/4 + U_b/8),$$

$$\alpha = \frac{\sqrt{2N}}{\Omega}(U_a/2 - U_b/8 + \mu_a/2N - \mu_b/4N), \tag{8}$$

θ is the phase difference between the modes, and z is the difference in populations. It is not difficult to transform the Hamiltonian (7) to the form (4) denoting $z=-w$ and introducing a new time variable $t'=4t/N$ to get rid of the $4/N$ multiplier in the last term of Eq. (7). The term β is not important for dynamics. Therefore, the Hamiltonian (4) describes coupled atomic-molecular BECs (with s-wave interactions) in the mean-field limit. Sweeping through Feshbach resonance can be modeled now by changing δ and keeping λ fixed in the Hamiltonian (4). The self-trapping phenomenon in the model discussed in [43] allows us to predict qualitatively a new effect—that is, the nonzero remnant fraction in the adiabatic passage through the resonance; we do not present a detailed quantitative analysis of the model in the present paper, but note that it may provide an alternative explanation of the finite conversion efficiency at the Feshbach resonance passage within the mean-field approximation. Similar to the approach of [26] mentioned above, s-wave interactions within molecular BECs can be included in the model of the fermionic-atom–Bose-molecule system via the same coefficient $\lambda \neq 0$ in (4).

Phase portraits with $\lambda=0$ (case I) and different values of δ are given in Fig. 1. Phase portraits with some constant $\lambda<0$ (case II) and different values of δ are given in Fig. 2. The phase portraits for case I were analyzed in detail in [27]. The dynamics can also be visualized using the variables u, v, and w of the system (5). The latter system possesses an integral of motion, $u^2+v^2-\frac{1}{2}(w-1)^2(w+1)=0$, defining the generalized Bloch sphere (see Fig. 4). The important property of the generalized Bloch sphere is the singular (conical) point at (0,0,1). As described in [27], the points $(0,0,\pm 1)$ are represented by the segments $w=\pm 1$ in the Hamiltonian phase portraits. Nevertheless, it does not mean that all points of either segment are equivalent. As described in [27,28], saddle points appear on the segment $w=1$ at certain values of the parameter δ. This drastically influence the dynamics in the vicinity of $w=1$. Let us briefly recall the description of the phase portraits previously given in [27].

If $\delta>\sqrt{2}$, there is only one stable elliptic point on the phase portrait, at $\theta=0$ and w not far from −1 [see Fig. 1(a)]. At $\delta=\sqrt{2}$ a bifurcation takes place, and at $\sqrt{2}>\delta>0$ the phase portrait looks as shown in Fig. 1(c). There are two saddle points at $w=1$, $\cos\theta=-\delta/\sqrt{2}$ and a newborn elliptic point at $\theta=\pi$. The trajectory connecting these two saddles points separates rotations and oscillating motions, and we call it the separatrix of the frozen system (what is most important is that the period of motion along this trajectory is equal to infinity). At $\delta=0$ on the phase portrait the segment $w=-1$ belongs to the separatrix [Fig. 2(d)]. At $0<\delta<\sqrt{2}$ the phase portrait looks as shown in Fig. 2(e). At $\delta=-\sqrt{2}$ the bifurcation happens, and finally, at large positive values of δ, again there is only one elliptic stationary point at $\theta=\pi$ and w close to −1.

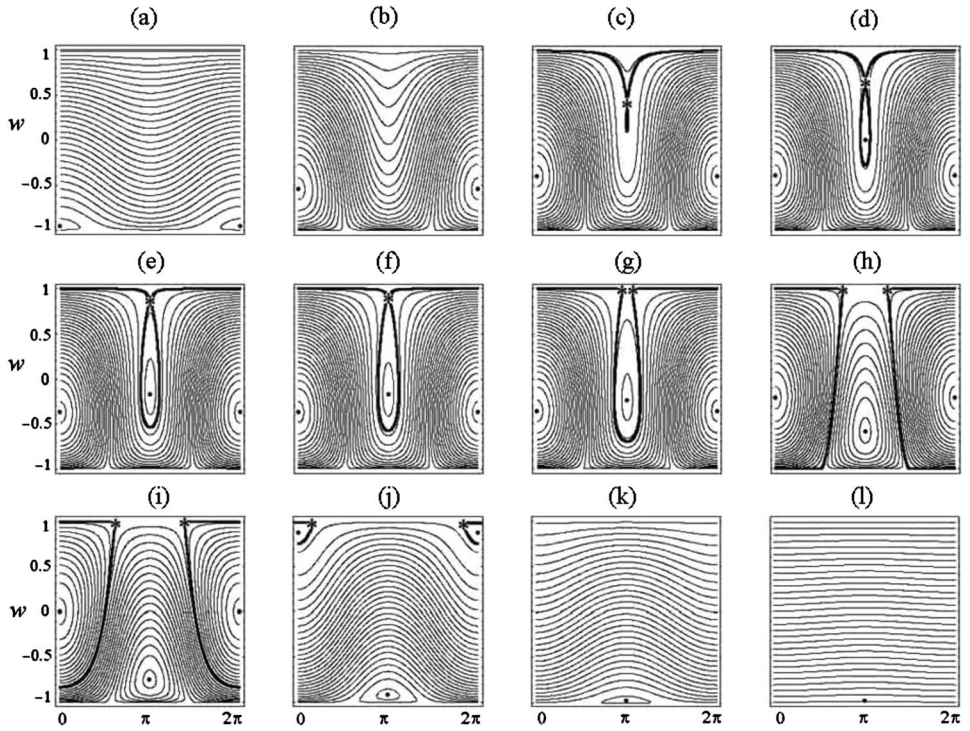

FIG. 2. Phase portraits of the Hamiltonian (4) with $\lambda<0$ ($\lambda=-0.5$). From upper left to bottom right (a)–(l): $\delta=5.0$, 1.0, 0.53, 0.5, 0.45, 0.44, 0.4, 0, −0.5, −2.2, −5, −50. In (c)–(f), the separatrix divide phase portraits on three domains $G_{1,2,3}$ (G_2 is adjacent to the segment $w=1$, G_1 is adjacent to $w=-1$, G_3 is the loop in between). Starting with small initial action at $w\sim 1$, a phase point undergoes a geometric jump in the action in addition to a dynamical jump. This leads to analog of nonzero AT and finite conversion efficiency in the adiabatic limit.

Let us introduce the action variable. Consider a phase trajectory on a phase portrait frozen at a certain value of δ. If the trajectory is closed, the area S enclosed by it is connected with the action I of the system by a simple relation $S=2\pi I$. If the trajectory is not closed, we define the action as follows. If the area S bounded by the trajectory and lines $w=1$, $\theta=0$, $\theta=2\pi$ is smaller than 2π, we still have $S=2\pi I$. If S is larger than 2π, we put $2\pi I=4\pi-S$. Defined in this way, I is a continuous function of the coordinates.

How does the process of Feshbach resonance passage happen in terms of the classical portraits of Fig. 1? Suppose one starts with $w(0)=w_0\approx 1$ and $\delta(0)\gg 1$ (physically, it means that almost all population is in the atomic mode, but there is small initial molecular fraction). In the phase portrait of the unperturbed system the corresponding trajectory looks like a straight line [Fig. 1(a)]. The initial action of the system approximately equals $1-w_0$. For example, assume that the area S_* within the separatrix loop in Fig. 1(c) (corresponding to $\delta=\delta_*=1$) is equal to $S_*=2\pi I_0=2\pi(1-w_0)$. When, as δ slowly decreases, the trajectory on an unperturbed phase portrait corresponding to the exact instantaneous position of the phase point $\{w(t),\theta(t)\}$ slowly deforms, but the area bounded by it remains approximately constant, the action is the approximate adiabatic invariant far from the separatrix [10]. As δ tends to δ_*, the form of the trajectory tends to the form of the separatrix loop in Fig. 1(c). The phase point is forced to pass near the saddle point at the $w=1$ segment many times. Since the area S within the separatrix loop slowly grows, approximately at the moment $\tau=\tau_*$ when $\delta(\tau_*)=\delta_*$ separatrix crossing occurs, and the phase point changes its regime of motion from rotational to the oscillatory around the elliptic point inside the separatrix loop. Then, it follows this elliptic point adiabatically (as no separatrix crossings occur anymore). The elliptic point reaches $w=-1$ at large positive δ. The value of the population imbalance tends to some final value $w=w_f$. The action variable at large δ is approximately equal to $1+w$. We see that in the adiabatic limit the sign of the population imbalance is reversed, $w_0=-w_f$. A nonadiabatic correction to this result arises due to the separatrix crossing and is discussed in detail in the next paragraph.

In case II the phase portraits have richer structure (Fig. 2). With $\lambda\neq 0$, another saddle point can appear at $\theta=\pi$ provided $\lambda<\lambda_c=-\frac{1}{2^{3/2}}$. The appearance of this saddle point can be understood from a graphical solution of the equation (see also [43])

$$2\lambda w-\delta=-\frac{3w+1}{2\sqrt{w+1}}. \tag{9}$$

As δ is decreased, the line $y(w)=2\lambda w-\delta$ goes up and crosses the curve determined by the right-hand side (rhs) of (9) (Fig. 3). Two points of intersection represent the saddle point (which moves to $w=1$ as δ is decreased further) and the elliptic fixed point which moves to $w=-1$. As the saddle point reaches the $w=1$ segment, another bifurcation occurs and the saddle point "splits" into two saddle points (similar to those in Fig. 1) that move apart from $\theta=\pi$ along the segment $w=1$ and disappear at $\theta=0$.

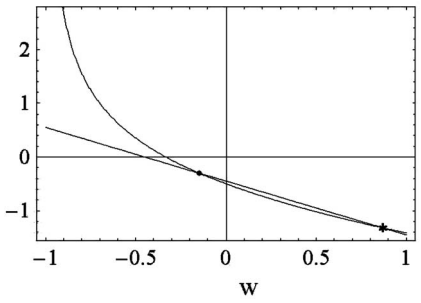

FIG. 3. Graphical solution of Eq. (9). The line $y(w)=2\lambda w-\delta$ crosses the curve $y(w)=-\frac{3w+1}{2\sqrt{w+1}}$ at two points (provided $2\lambda<\max\{y'(w)\}=-1/\sqrt{2}$), one of the points corresponding to the unstable fixed point on the phase portraits of Figs. 2(c)–2(f), while the other to the stable elliptic point at $\theta=\pi$. As δ decreases further, the unstable fixed point moves to $w=1$.

In Sec. II B the dynamical change in the action in the case $\lambda=0$ is considered in detail, while Sec. II C briefly discusses the case $\lambda\neq 0$ (geometric jump).

B. Case I: Negligible mean-field interactions, $\lambda=0$, dynamical change in the action at the separatrix crossing

Consider in greater detail the passage through the separatrix in Fig. 1 described in the previous subsection. At large positive δ, $1-w$ is proportional to the classical action, while at large negative δ action is proportional to $1+w$ (see also Fig. 4). In the adiabatic limit, w reverses its sign due to passage through the resonance: the final and initial values of w are related as $w_f=-w_{in}$. Calculating the change in the action due to separatrix crossing (Refs. [27,28]), one obtains the nonadiabatic correction to this adiabatic result. It scales linearly with ϵ if the initial population imbalance slightly deviates from 1 (i.e., the initial molecular fraction is not very small).

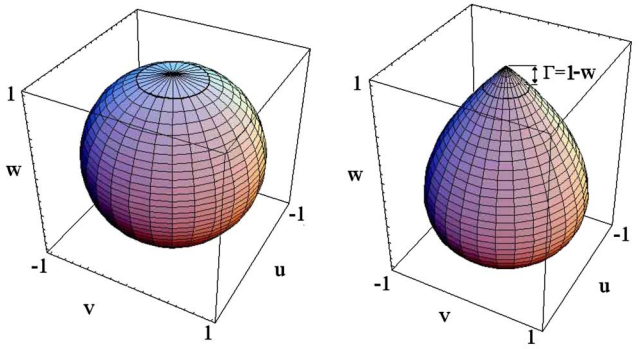

FIG. 4. (Color online) The Bloch sphere corresponding to ABEC models and the generalized Bloch sphere corresponding to AMBEC models [the surfaces $u^2+v^2=1-w^2$ on the left and $u^2+v^2=\frac{1}{2}(w-1)^2(w+1)$ on the right]. At large detuning, near $w=1$, the area within a trajectory on the generalized Bloch sphere is proportional to $u^2+v^2\approx(1-w)^2=\Gamma^2$, while on Bloch sphere the area is proportional to $u^2+v^2\approx 2(1-w)=2\Gamma$. Note, however, that the action variable in either case is proportional to $1-w$. Action is related to the area on the Hamiltonian phase portraits which is approximately equal to $1-w$ for the corresponding trajectory; see [27,28].

As the trajectory nears the separatrix due to a slow change (of order ϵ) in the parameter, the action undergoes oscillations of order of ϵ. Each oscillation corresponds to one period of motion of the corresponding trajectory in the unperturbed system. In the vicinity of the separatrix, the period of motion grows logarithmically with energy difference h between energy level of the unperturbed trajectory and the energy on the separatrix (so as h tends to 0, the period of motion tends to infinity). As a result, the "slow" change of the parameter becomes "fast" as compared to the period of motion: a breakdown of adiabaticity happens; oscillations of the adiabatic invariant grow and at the crossing its value undergoes a quasirandom jump (Fig. 5).

According to the general theory, it is not enough to consider dynamics of the action variable. One introduces the improved adiabatic invariant $J=I+\epsilon f(w,\theta,\tau)$ (see Appendix A for a brief description of the adiabatic and improved adiabatic approximations and the general formula for J). The improved adiabatic invariant is conserved with better accuracy: far from the separatrix, it undergoes very small oscillations of order ϵ^2. At the separatrix crossing, it undergoes jump of order ϵ.

We illustrate this behavior in Fig. 5. Figures 5(a) and 5(b) give the dynamics of the action (adiabatic invariant) I. It is clearly seen that before and after separatrix crossing it oscillates around different mean values, but the jump in action is of the same order as its oscillations close to the separatrix. Figure 5(c) presents the time evolution of the improved adiabatic invariant. The jump in J is much more pronounced (although it is possible to express the improved adiabatic invariant in the elliptic functions, we choose to calculate it numerically according to the definition given in Appendix A).

Now, at large $|\delta|$ not only the action I coincides with the value of $1-|w|$, but also the improved adiabatic invariant J coincides with I. Therefore, calculating the change in the improved adiabatic invariant J, we obtain the change in the action and change in the value of $1-|w|$ due to the resonance passage. For the case of small initial action I, the change in action was calculated in [27] according to the general method of [10]. The formula is

$$2\pi\Delta J=-2\frac{\epsilon\Theta_*}{\sqrt{2-\delta_*^2}}\ln(2\sin\pi\xi), \tag{10}$$

where Θ is the rate of change of the area within the separatrix loop: $\Theta=\frac{dS}{d\tau}$ (note that the rate does not depend on ϵ); ξ is the pseudophase: $\xi=|h_0/\epsilon\Theta|$, where h_0 is the value of the energy at the last crossing the vertex bisecting the angle between incoming and outgoing separatrices of the saddle point C outside the separatrix loop [see Fig. 1(c)]. Similar calculations were done in [20]. The formula can be further simplified by expressing Θ via $\frac{\partial\delta}{\partial\tau}\equiv\delta'$. Indeed, the area within the separatrix loop is $S(\delta)=2\int_{\delta^2-1}^{1}dw\left[\pi-\arccos\left(\frac{\delta}{\sqrt{1+w}}\right)\right]$. We are interested in the derivative of $S(\delta)$ over δ. Differentiating the above integral over the parameter δ, one obtains

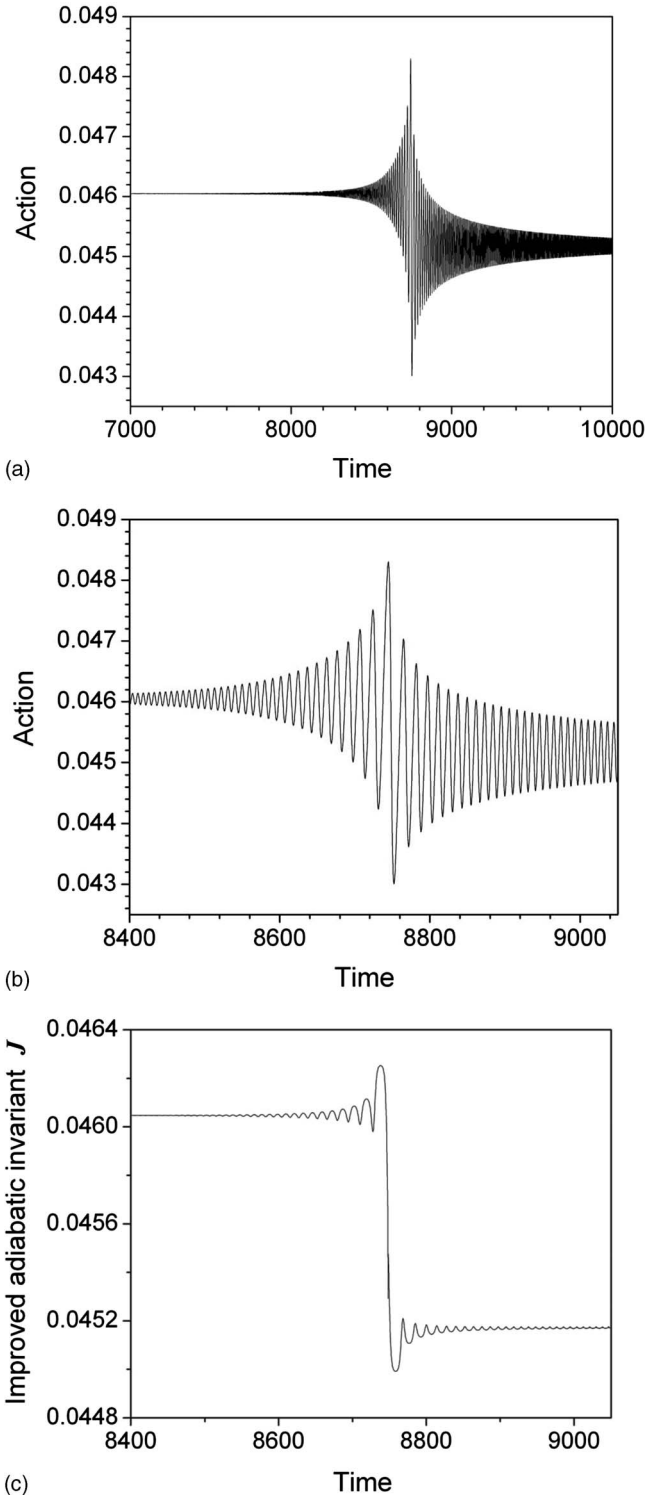

FIG. 5. Time evolution of the adiabatic invariant (action) I and the improved adiabatic invariant J in the model (4) with $\lambda=0$.

$$S'(\delta)=4\sqrt{2-\delta^2},\quad \Theta=S'(\delta)\frac{\partial\delta}{\partial\tau}=S'(\delta)\delta'. \tag{11}$$

Therefore, the formula (10) is simplified to

$$\Delta J=-\frac{4\epsilon\delta'}{\pi}\ln(2\sin\pi\xi). \tag{12}$$

We carefully checked numerically the behavior of jumps in the action predicted by formula (12); see Fig. 6. Figure 6(a) demonstrates scattering at the separatrix crossing: the bunch of trajectories with various (but close) initial conditions undergoing jumps of the improved adiabatic invariant at separatrix crossing. Figures 6(b) and 6(c) demonstrate the ϵ dependence of jumps of the improved adiabatic invariant. For several values of ϵ, a bunch of 80 trajectories with close initial conditions was calculated, and the dispersion of actions due to separatrix crossing was calculated, which scales linearly with ϵ^2 (i.e., $\sigma^2=K\epsilon^2$). Note that from the formula (12) it is possible to determine not only the linear power law, but also the corresponding coefficient of proportionality, K. The theory predicts a uniform distribution of ξ; therefore the dispersion of jump in the action can be calculated as

$$\sigma^2=16\epsilon^2(\delta')^2\pi^{-2}\int_0^1\ln^2 2\sin\pi\xi d\xi=\frac{4\epsilon^2(\delta')^2}{3}. \tag{13}$$

For numerical calculations, we used a linear sweeping of δ; therefore, the predicted dispersion is $\sigma^2=4\epsilon^2/3$. The predicted coefficient $4/3$ can be compared with the slope in Figs. 6(b) and 6(c). For relatively large ϵ [Fig. 6(b)], the correspondence is not very good, but when we decreased the value of ϵ, we obtained $K\approx 1.348$ which is in good correspondence with the theoretically predicted $K=4/3\approx 1.333$. We reveal also a high sensitivity of the jump of the adiabatic invariant on initial conditions [Fig. 6(d)], which is the cause of uniform distribution of ξ [10]. We therefore checked almost all qualitative and quantitative aspects of the destruction of adiabatic invariance at separatrix crossings in that model. Let us finally mention the main steps in obtaining the formula.

(i) Linearization around the saddle point in the frozen system and derivation of a approximate formula for the period of motion T along the trajectory with energy h. The period depends logarithmically on h and is inversely proportional to the square root from the Hessian of the Hamiltonian in the saddle point (determinant of the matrix of second derivatives).

(ii) Obtaining the action variable I from the period T using the formula $T=2\pi\partial I/\partial h$.

(iii) Calculation the function f at a point of the vertex bisecting the angle between incoming and outgoing separatrices of the saddle point [Fig. 1(c)]. It is proportional to Θ (for details, see [10]).

(iv) "Slicing" the exact trajectory on parts (corresponding to "turns" in the unperturbed system) by the bisecting vertex and constructing a map $\tau_n, J_n\to\tau_{n+1}, J_{n+1}$ using the analysis described above (τ_0 is the moment of last crossing of the vertex before the separatrix crossing, τ_{-1} is a previous moment of crossing the vertex, etc., and J_n is value of the improved adiabatic invariant at τ_n). Summation of the changes of the adiabatic invariant at each turn leads to the formula (12).

See Refs. [27,28] for further details.

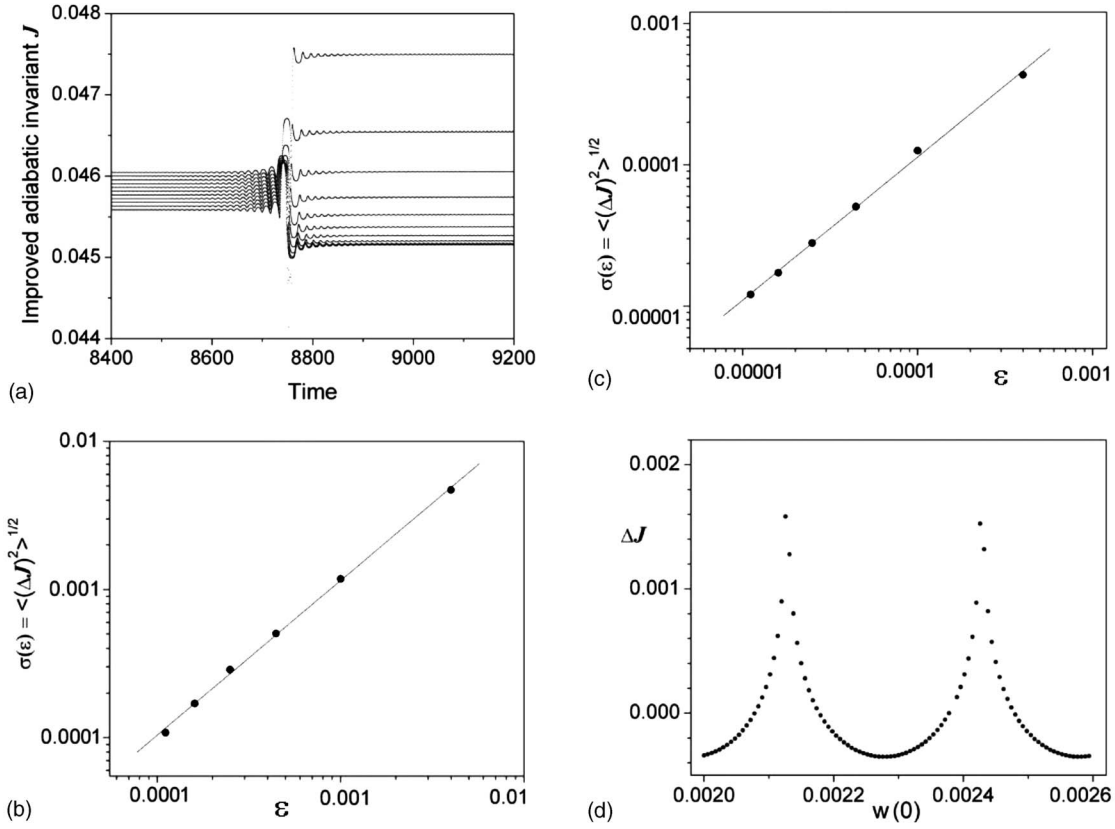

FIG. 6. Scattering at the separatrix crossing. (a) Bunch of trajectories with various (but close) initial conditions undergoing jump of the improved adiabatic invariant at separatrix crossing. Trajectories are mixed due to the jumps. (b) ϵ dependence of magnitude of jump of the improved adiabatic invariant. For every value of ϵ, we calculated a bunch of 80 trajectories from $\delta=10$ to $\delta=0$. Initial values of w were chosen to be equidistantly distributed in the interval $[0.96, 0.96+1.5\epsilon]$. The theory predicts a quasirandom jump of the improved adiabatic invariant, the magnitude of which scales linearly with ϵ. We calculate the mean value σ of the squared change in the improved adiabatic invariant, which turns out to scale perfectly linearly with ϵ (accordingly, the dispersion σ^2 scales linearly with ϵ^2). (c) The same as in (b), but with smaller values of ϵ and initial values of action. We calculated slope of the line $\sigma(\epsilon)$ taking into account the four points with the smallest values of ϵ and get the value $k\approx 1.1614$, which is in good correspondence with theoretical prediction of $\sqrt{4/3}\approx 1.15$; for larger values of ϵ, the correspondence worsens: $k\approx 1.015$ when taking into account all points. (d) High sensitivity of the jump of the adiabatic invariant on initial conditions. Calculations for $\epsilon=0.0004$ are presented. Initial values of w for 100 trajectories were uniformly distributed in the tiny interval $(w_0, w_0+1.5\epsilon)$. Change in the improved adiabatic invariant was calculated $[\Delta J=J(\delta=0)-J(\delta=10)]$. It is seen that a tiny change in the initial conditions results in a large variance of the jump of the action. Trajectories arrive at the separatrix with different values of the pseudo phase ξ. Maxima in the figure correspond to $\xi=0$ and $\xi=1$. The formula for the jump of the adiabatic invariant predicts a high increase in the value of the jump when $\sim(\pi\xi)$ nears 0. In the very vicinity of $\xi=0,1$ the formula is not working (the predicted jump diverges while the calculated jump is finite); however, the measure of the exceptional initial conditions leading to $\xi=0,1$ is very small [10].

C. Case II: Condensates with interactions, $\lambda\neq 0$, analog of nonzero adiabatic tunneling

Let us briefly consider the model with $\lambda<\lambda_c=-\frac{1}{2^{3/2}}$. Separatrix crossing happens via another scenario here (according to the motion of the fixed points described in Sec. II A). We give only a qualitative discussion of a possible new phenomenon. We plot the phase portraits at different δ and fixed λ in Fig. 2. Now, as δ is decreased, three domains $G_{1,2,3}$ appear in the phase portrait at certain $\tau=\tau_*$ as a result of the first bifurcation. Shortly after the bifurcation [see Fig. 2(c)] the separatrix consists of two "loops:" the upper G_2 (adjacent to $w=1$ line), which area $S_2(\tau)$ decreases from $S_2(\tau_*)$ to zero as the unstable fixed point goes towards $w=1$, and the bottom G_3, whose area $S_3(\tau)$ increases from zero; G_1 is the "outer" domain adjacent to $w=-1$.

In the case where the initial action I_0 of a phase point is sufficiently small $[2\pi I_0<S_2(\tau_*)]$, the phase point resides in the G_2 domain when the separatrix emerges [without any separatrix crossing; see Fig. 2(c)]. In the case where $2\pi I_0$ is larger than the area S_2 of the domain G_2 at the moment of separatrix creation, the phase point occupy G_1 at this moment. Consider the former case—i.e., small initial action. As δ evolves, S_2 decreases, while S_3 grows. When $S_2(t)$ becomes equal to $2\pi I_0$, separatrix crossing occurs and the phase point is expelled to the G_1 domain and then almost immediately to the G_3 domain [say, in Fig. 2(f)]. It is easy to see that the phase point acquires a large action due to the geometric jump in the action when entering G_3, so in the end w will deviate from the all-molecule mode $w=-1$ considerably (the geometric jump is equal to $[S_3(\tau_{**})-S_2(\tau_{**})]/2\pi$, where τ_{**} is

the moment of the separatrix crossing). This is in some sense analogous to the *nonzero AT* discussed in [24,25] and in Sec. III of the present paper. One might try to explain the sizable remnant fraction after the adiabatic Feshbach resonance passage as the geometric jump in the action due to the self-trapping effect of *s*-wave interactions. This, however, requires further investigation: while calculation of the geometric jump in action is trivial, the dynamical jump is not so easy to calculate in this geometry. So far, we just suggest a possible new phenomenon in the model; a detailed discussion will be given elsewhere.

III. NONLINEAR TWO-MODE MODEL FOR TWO COUPLED BECs

A. Model equation and its physical origin: Phase portraits

We consider the Hamiltonian ("nonlinear two-mode ABEC model")

$$H = -\delta w + \frac{\lambda w^2}{2} - \sqrt{1-w^2}\cos\theta. \tag{14}$$

There are many systems in BEC physics that are described in the mean-field limit by the Hamiltonian (14). It has been used to model two coupled BECs (BEC in a symmetric double well in case $\delta=0$) [23]. The model with $\delta \neq 0$ is equivalent to nonlinear Landau-Zener model, which appears, in particular, in studying BEC acceleration in optical lattices [24,25].

The theory of nonlinear Landau-Zener tunneling was suggested in [24,25]. However, only the case of zero initial action was considered. In particular, it is said in [25] that adiabaticity is broken when "fixed points collide." In the case where the initial action is not zero, adiabaticity is broken before that: it is broken when separatrix crossing occurs. Therefore, it is necessary to involve the theory of separatrix crossings in consideration of these models.

It is worth mentioning that for BECs in a symmetric double well, there exists also an improved two-mode model [38], where the term $\cos 2\theta$ is added:

$$H = A\frac{z^2}{2} - B\sqrt{1-z^2}\cos\theta + \frac{1}{2}C(1-z^2)\cos 2\theta, \tag{15}$$

where the parameters A, B, and C are determined by overlap integrals of the mode functions. Usually, the $\cos 2\theta$ term is small and can be omitted. Then, the improved model Hamiltonian can be reduced to Eq. (14) with $\delta=0$ (still, the coefficients are determined more accurately in the improved model). The original model is derived for the case of constant parameters. One may wonder if it is working in a time-dependent situation. It is not difficult to demonstrate that for slowly changing parameters one can use the same model, with parameters of the Hamiltonian slowly changing in accordance with the "instantaneous" model. For simplicity, let us demonstrate this using the improved two-mode model [38] as an example. The order parameter in a two-mode approximation is

$$\psi(x,t) = \sqrt{N}[\psi_1(t)\Phi_1(x) + \psi_2(t)\Phi_2(x)],$$

$$\Phi_{1,2}(x) = \frac{\Phi_+(x) \pm \Phi_-(x)}{\sqrt{2}}, \tag{16}$$

where $\Phi_\pm$ satisfy the stationary GP equation

$$\beta_\pm \Phi_\pm = -\frac{1}{2}\frac{d^2\Phi_\pm}{dx^2} + V_{\text{ext}}\Phi_\pm + g|\Phi_\pm|^2\Phi_\pm. \tag{17}$$

The variables of the classical Hamiltonian are defined as

$$z(t) = |\psi_1(t)|^2 - |\psi_2(t)|^2, \quad \phi(t) = \arg\psi_2(t) - \arg\psi_1(t). \tag{18}$$

Substituting Eqs. (16) and (17) into the time-dependent GP equation, one gets [38]

$$i\frac{d\psi_1(t)}{dt}(\Phi_+ + \Phi_-) + i\frac{d\psi_2(t)}{dt}(\Phi_+ - \Phi_-) = \Sigma_\pm(\psi_1(t) \pm \psi_2(t))[\beta_\pm - gN|\Phi_\pm|^2]\Phi_\pm + \frac{gN}{2}\Sigma_\pm[\Phi_\pm^3 P_\pm + \Phi_\pm^2\Phi_\mp Q_\pm], \tag{19}$$

where $P_\pm$, $Q_\pm$ are functions of ψ_1, ψ_2 (see [38]). From these equations, one get the equations of motion for ψ_1, ψ_2 [Eq. (13) from [38]]:

$$i\dot{\psi}_\mu = \left(F + A|\psi_\mu|^2 - \frac{\Delta\gamma}{4}\psi_\mu\psi_\nu^*\right)\psi_\mu + \left(-\frac{\Delta\beta}{2} + \frac{\delta\gamma}{4}|\psi_\mu|^2 + C\psi_\mu^*\psi_\nu\right)\psi_\nu, \tag{20}$$

which can be rewritten as a Hamiltonian equation of motion of the corresponding classical pendulum (F, A, C, $\Delta\gamma$, $\Delta\beta$ are functions of mode overlap integrals and energies $\beta_\pm$). Considering time-varying parameters, we introduce the instantaneous mode functions $\Phi_\pm(x,t)$. If we keep the two-mode expansion of the order parameter, then it is not difficult to show that additional terms coming from the time dependence of the mode functions ($\int\Phi_+\frac{\partial\Phi_+}{\partial t}d\mathbf{r}$, $\int\Phi_+\frac{\partial\Phi_-}{\partial t}d\mathbf{r}$, etc.) are strictly zero due to symmetry and normalization conditions. Complications can arise only from excitation of other modes (if we would allow, say, four-mode expansion). However, we do not consider this question here. Even in the two-mode approximation the nonadiabatic dynamics is nontrivial, and it comes purely from the nonadiabatic behavior of classical action. Phase portraits of the model (14) with $\delta=0$ are given in Fig. 7. We are interested only in the supercritical case here. Separatrix crossings and corresponding changes in the action are discussed in Sec. II B. The case $\delta \neq 0$ (NLZ model) is discussed in Sec. II C, where we present the phenomenon of *separated AT*.

B. Case I: Symmetric double well, $\delta=0$

We suppose initially that the system is in the oscillating regime of complete tunneling oscillations (domain G_3) and then, due to a slow change of parameters, is switched into the self-trapped regime. Two different probabilistic phenomena take place at the crossing: a quasirandom jump in the action and probabilistic capture.

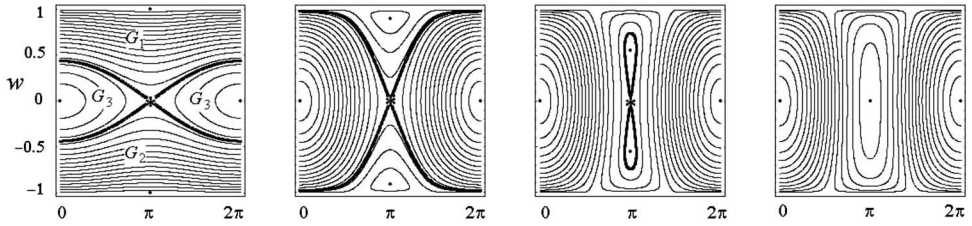

FIG. 7. Phase portraits of the two-mode ABEC Hamiltonian with $\delta=0$. From left to right (a), (b), (c), (d): $\lambda=20, 2.4, 1.2, 0.8$. As λ decreases, separatrix loop grows until $\lambda=2$ where it changes its configuration, and at $\lambda=1$ it disappears. On the other hand, by increasing λ it is possible to switch from regime of complete oscillations (domain 3) to the self-trapped regime (domain 1 or 2). The unstable fixed point do not move: it is either at (0,0) or absent.

Consider the probabilistic capture: there are two domains $G_{1,2}$ for the self-trapped regime in the phase portraits: in the first (upper) $w>0$ and in the second (bottom) $w<0$. In which of these two domains will the phase point be trapped (in other words, in the left or the right well)? The trapping in either of the domains is also very sensitive to initial conditions; in the limit of small ϵ, the trapping is a probabilistic event. For the symmetric case, the probability to be trapped in either well is exactly 1/2. However, for the asymmetric well the answer is not so straightforward. It is determined by some integrals over the separatrix at the moment of switching (general theory exists; see [10]).

As for the first phenomenon (jump in the action), at the moment of switching, destruction of adiabaticity happens in the sense that the adiabatic invariant undergoes a relatively large jump of order of $\sqrt{\epsilon}$ (very similar to that discussed in the Sec. II). If we then slowly bring the parameters back to the initial values, the adiabatic invariant will be different.

The formulas for the action-angle variables are cumbersome. In fact, to calculate change in the action, it is not necessary to have formulas for the action-angle variables. The jump is determined by local properties of the Hamiltonian near the separatrix: the area of the separatrix loop and the Hessian of the unstable fixed point [10]. As a result, the formula for the jump of the action is simpler than expressions for the action itself. Suppose $\lambda>2$ so that the phase portrait looks like in Fig. 7(b) and we start from the regime of complete oscillations. Slowly changing λ, we can switch to the self-trapped regime. The expression for the area of the separatrix loop is easy to calculate:

$$S(\tau)/4 = b + \arcsin b, \quad b = \frac{2\sqrt{\lambda-1}}{\lambda}. \tag{21}$$

The Hessian of the Hamiltonian in the unstable fixed point can be calculated as $D(\tau)=-(\lambda-1)$.

Let us define

$$d(\tau) \equiv 1/\sqrt{-D(\tau)}. \tag{22}$$

We calculated jump of the action according to the general method as

$$\Delta J = -\frac{1}{2\pi}\epsilon d_* \Theta_* \ln[2\sin(\pi\xi)] = \epsilon\frac{4\lambda'}{\pi\lambda^2}\ln[2\sin(\pi\xi)], \tag{23}$$

where ξ is the pseudophase corresponding to the first crossing of line $\theta=\pi$ in the $G_{1,2}$ domains, d_* is value of d at the moment of crossing this line, and values of λ and λ' are also taken at this moment.

We checked this formula numerically. A set of 100 phase points with initial conditions being distributed in a small (of order ϵ) interval far from the separatrix was chosen. Then, the bunch of trajectories in the system with slowly changing parameter was calculated. For each trajectory, values of ξ and ΔJ (change in the improved adiabatic invariant) were determined. From numerically determined ξ, the theoretical prediction for change in the action ΔJ was calculated and compared with numerically determined ΔJ. Results are in the Fig. 8; the correspondence between numerical results and analytical prediction is perfect. In the same calculations, mechanism of quasirandom division of phase flow was verified: exactly one-half of the phase points from the considered set were captured in the upper domain G_1, and the other half were trapped in the lower domain G_2. This is a purely classical phenomenon, the sound example of probabilistic phenomena in dynamical systems [10,48].

C. Case II: Asymmetric double-well and nonlinear Landau-Zener model, $\delta\neq 0$

Consider sweeping value of δ from large positive to large negative values in Fig. 9 (see also [24,25]). In the case $\lambda<1$, only two fixed points exist at $\theta=0,\pi$ (P_2, P_1 correspondingly). As δ changes from $\delta=-\infty$ to $\delta=+\infty$, P_1 (corresponding to the lower "eigenstate") moves along the line $\theta=\pi$ from the bottom ($w=-1$) to the top ($w=1$); the other point P_2 (corresponding to the upper "eigenstate") moves from the top to the bottom. In the case $\lambda>1$, two more fixed points appear in the window $-\delta_c<\delta<\delta_c$, $\delta_c=(\lambda^{2/3}-1)^{3/2}$. We concentrate on this, "above-critical" case. The new points lie on the line $\theta=\pi$, one being elliptic (P_3) and the other hyperbolic (P_4). Again, it is convenient to use graphical solution (Fig. 10) to visualize the appearance and disappearance of the fixed points. It is stated in [25] that a collision between P_1 and P_3 leads to nonzero AT from the lower level to the upper level and the tunneling probability in the

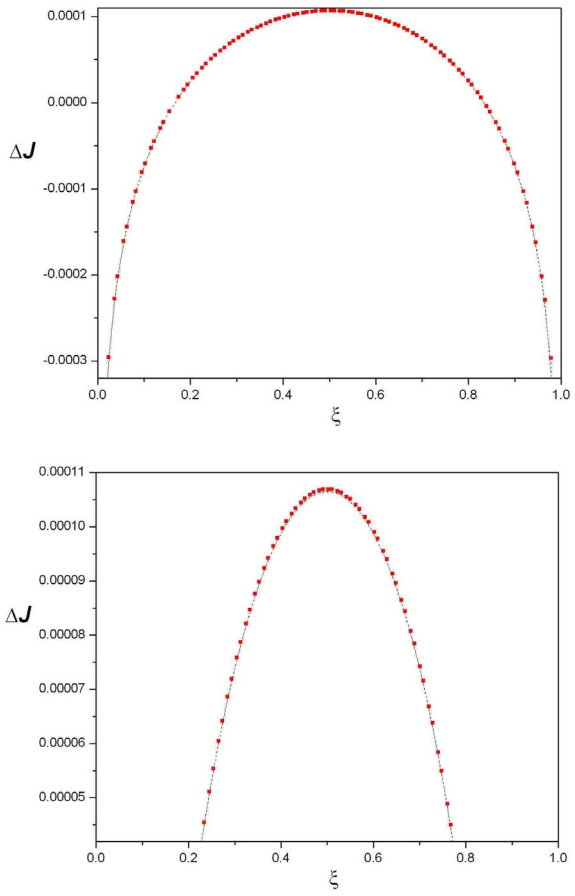

FIG. 8. (Color online) Jump in the improved adiabatic invariant in dependence of the pseudophase ξ. Solid squares, numerical results; dashed line, analytical predictions according to Eq. (23). We slowly changed λ according to the law $\lambda=\lambda_a-\lambda_b\cos\epsilon t$, with $\epsilon=0.001$, $\lambda_a=15$, $\lambda_b=10$. We took a set of 100 phase points with different but very close initial conditions: $w_i=0$, θ_i are distributed along an interval of order of ϵ at the time $\tau=\epsilon t=0$. We propagate the bunch of trajectories until the time $\tau=\pi$ (so all the points changed its regime of motion from complete oscillations to the self-trapped mode). For each point, the value of ξ and change in the improved adiabatic invariant ΔJ were determined numerically; then, the analytical prediction for the change in the improved adiabatic invariant $\Delta J(\xi)$ was calculated according to Eq. (23). The numerical and analytical results shown in (a) are almost indiscernible. In (b) an enlarged part of the same plot is presented, where small deviations are seen. It is also important to mention that from 100 phase points exactly 50 were trapped in the upper domain G_1 and 50 in the lower G_2.

adiabatic limit is obtained by calculating phase space area below the "homoclinic trajectory" (which is the limiting case of the separatrix with $S_3=0$)—i.e., as the *geometric* jump in the action. In the zeroth-order approximation, this approach is correct (if the initial action is zero or very small). It is very important that we can adopt the general theory of separatrix crossings to the case of this model with nonzero initial action (corresponding to initially excited system). In this case destruction of adiabaticity happens *before* collision of the phase points. The initial trajectory is almost a straight line, so the initial action is equal to $w+1$ in the case where we start close to $w=-1$ or $1-w$ in the case where we start close to $w=1$. Consider the former case. Let the initial action I_0 [i.e., value of $w+1$ in Fig. 9(a)] be equal to the area of the separatrix loop in Fig. 9(g). The phase point is oscillating around slowly moving P_1 point until the area of the separatrix loop $S_1(\tau)$ becomes equal to $2\pi I_0$ at some moment $\tau=\tau_*$, where separatrix crossing occurs. The action undergoes a geometric jump (which is simply $[S_3(\tau_*)-S_1(\tau_*)]/2\pi$). This geometric jump is the analog of the AT probability discussed in [24,25] for the case of zero initial action. The geometric jump is accompanied by a *dynamical* jump similar to that discussed in Secs. II and III B. The dynamical jump is small (of order of ϵ) as compared to the geometric jump. But conceptually it is very important: only the dynamical jump leads to destruction of the adiabatic invariance in the model. Indeed, if we reverse the change in δ, the phase point will return to its initial domain and the geometric jump will be completely canceled. However, dynamical jumps will not be canceled, and at multiple separatrix crossings they lead to slow chaotization (see, for example, [19]). Formulas for the dynamical jumps in the asymmetric case are more complicated, as there are terms of order ϵ and $\epsilon\ln\epsilon$. However, the probabilistic capture in this case is very much different. Consider the phase portraits in Figs. 9(f) and 9(g). Suppose that not only δ, but also λ is changing. At the moment of crossing, the area S_3 is diminishing, while the areas $S_{1,2}$ can behave differently depending on the evolution of the parameters. Suppose both $S_{1,2}$ are increasing: $\Theta_{1,2}>0$, $\Theta_3<0$. Denote as $l_{1,2}$ the parts of the separatrix below and above the saddle point, correspondingly. There is phase flow across l_2 from the domain G_2 to G_1 and across l_1 from G_3 to G_2. The latter flow is divided quasirandomly between G_2 and G_1: the phase point leaving G_3 can remain in G_2 or be expelled to G_2. This is "determined" during the first turn around the separatrix. After that, the particles are trapped either in G_1 or G_2. The probability for either event can be calculated as integrals over the separatrix parts $l_{1,2}$ [10]:

$$\mathcal{P}_1=\frac{I_2-I_1}{I_1},\quad \mathcal{P}_2=\frac{I_2}{I_1},$$

$$I_i(\delta,\lambda)=\oint_{l_i}dt\frac{\partial\bar{H}}{\partial\rho}=\oint_{l_i}dt\left(\frac{\partial H}{\partial\rho}-\frac{\partial H_s}{\partial\rho}\right),\quad \rho=\epsilon t. \quad (24)$$

Here integrals are taken along the unperturbed trajectories at the moment of separatrix crossing (or last crossing the line $\theta=\pi$ before the separatrix crossing), H_s is the (time-dependent) value of the Hamiltonian H in the unstable fixed point, and $\bar{H}$ denotes the Hamiltonian H normalized in such a way as to make the value of the new Hamiltonian in the unstable fixed point to be zero. It is possible to calculate all the integrals analytically; see Appendix B. We present a numerical example in Fig. 11. A set of $N=100$ trajectories was considered with initial conditions distributed in a tiny interval of w and with $\theta(0)=0$ (so the initial actions were distributed in a tiny interval of order ϵ: $I_k=I_0+k\delta I$, $N\delta I\sim\epsilon$, k

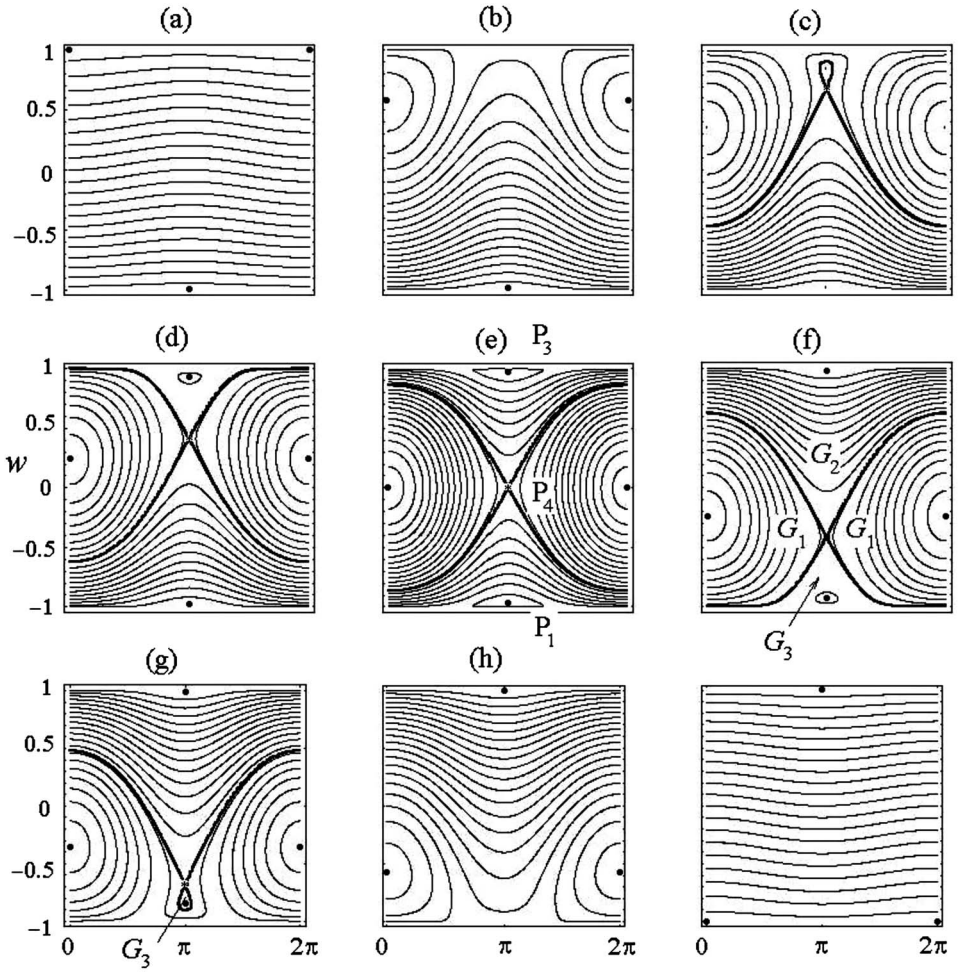

FIG. 9. Nonlinear Landau-Zener tunneling: phase portraits of the two-mode ABEC Hamiltonian at different values of δ. From top left to bottom right: $\delta=20$, 3, 1.8, 1.2, 0, −1.2, −1.8, −3, −20; $\lambda=\text{const}=4$.

$=1,\ldots,N$; alternatively, one can consider a set of phase point with equal initial actions, but with distribution of phase along 2π interval). Both δ and λ were changed, so after the separatrix crossing a phase point can be trapped either in G_1 or G_2. From the set of 100 points, 87 were trapped in G_1, while 13 were trapped in G_2. The difference between the final actions of these two subsets is approximately I_0, the initial action of points in the bunch. The probability of 87% is in good correspondence with the theoretical prediction, which gives $P_2=86.998$ for the probability of capture into the domain G_2. Possible experimental realization of this phenomenon is again BEC acceleration in optical lattices, but with simultaneous modulation of the lattice potential depth.

IV. CONCLUSION

We discussed destruction of adiabatic invariance in several nonlinear models related to BEC physics. We especially concentrated on the cases that have not been considered in the corresponding papers on BEC dynamics yet: that is, when the initial action is not zero.

We found that the general theory of adiabatic separatrix crossings works very well in the considered models. Two aspects of destruction of adiabatic invariance were considered: quasirandom jumps in the approximate adiabatic invariants and quasirandom captures in different domains of motion at separatrix crossings.

We discussed quasirandom jumps in the approximate adiabatic invariants in the models describing Feshbach resonance passage in coupled atom-molecule BECs, BEC tunneling oscillations in a double well, and nonlinear Landau-Zener tunneling. Comparing with previous analysis of the above-mentioned models [25,26], the key feature of our approach should be emphasized: the system is linearized near the hyperbolic fixed point, not near elliptic fixed points of the unperturbed system.

Another important class of phenomena considered here is probabilistic captures into different domains of motion. They were discussed for the case of BEC tunneling oscillations in a (symmetric or asymmetric) double well and the NLZ model with a time dependence of the nonlinearity λ. *Separated AT* was discovered in the latter case. We suppose it can have experimental applications in BEC manipulations with optical lattices. The conceptual phenomenon of probabilistic capture was first discovered in celestial mechanics (while studying resonance phenomena in the Solar System). It is

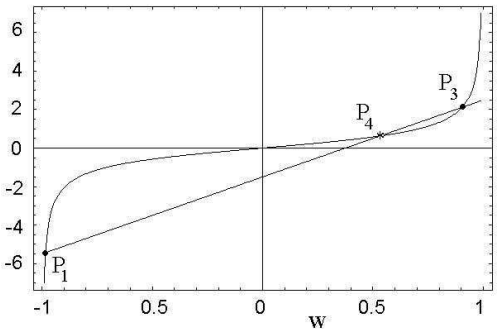

FIG. 10. Graphical solution of the equation $-\delta+\lambda w = w/\sqrt{1-w^2}$ which gives fixed points at $\theta=\pi$. As δ decreases, the line goes up, and three fixed points can appear from a single one at certain window of value of δ provided $\lambda>1$. The star denotes the unstable fixed point which after the birth goes down and collides with the stable fixed point. See corresponding phase portraits in the next figure.

interesting to draw an analogy between intricate phenomena of celestial dynamics and phenomena happening in many-body quantum systems. Conceptual phenomena related to the classical adiabatic theory [which includes both adiabatic invariants and the adiabatic (geometric) phases] have recently become an important trend of research in the highly interdisciplinary BEC physics field (see [28,58–60]). We hope the comprehensive analysis presented in this paper adds an important contribution to the understanding the nonlinear dynamics of Bose-Einstein condensates.

Note added in proof. Recently, several papers have appeared [61] that have studied the classical phenomena described here. It is necessary to mention a work [62] where a careful discussion of the self-trapping effect was given.

ACKNOWLEDGMENTS

A.P.I. was supported by JSPS. A.P.I. thanks D. Feder and A. Perali for their help during participation in the BCAM05 meeting and NQS-2005 conference correspondingly, where part of this work was presented. Encouraging short discussions with R. Hulet, M. Oberhaler, E. Arimondo, and W. Ketterle are acknowledged. Many thanks to A. A. Vasiliev and A. I. Neishtadt for clarifying discussions and help in the calculations. The authors thank O. I. Tolstikhin, S. Dmitriev, Y. Kivshar, and K. Nakagawa for discussions. This work was supported also by Grants-in-Aid for Scientific Research Nos. 15540381 and 16-04315 from the Ministry of Education, Culture, Sports, Science and Technology, Japan, and also in part by the 21st Century COE program on "Coherent Optical Science."

APPENDIX A: ADIABATIC AND IMPROVED ADIABATIC APPROXIMATIONS

To consider the change in the action during a separatrix crossing, it is necessary to introduce the improved adiabatic invariant J in addition to the ordinary action variable I. The improved adiabatic approximation is discussed in [10].

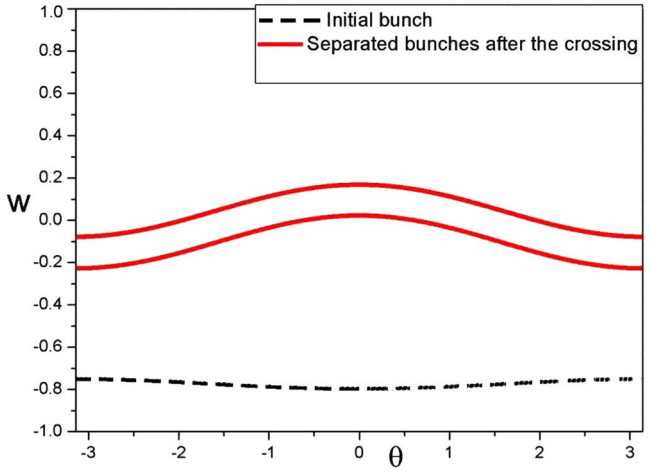

FIG. 11. (Color online) Separated AT. We took a bunch of 100 trajectories with initial actions distributed in a tiny interval of order ϵ [in the figure, the bottom curve (dashed) consists of 100 initial trajectories; the two upper curves (solid line) consist of 87 and 13 trajectories, correspondingly, and represent "snapshot" of the trajectories after the end of sweeping of parameters]. As parameters are changing, the separatrix [see Figs. 9(d)–9(f)] moves down and crosses the bunch. Due to quasirandom division of phase flow described in the text, some of the points were captured to the G_1 domain, while the other to the G_2 domain. As a result, phase points undergo different geometric change in the action. After the capture, actions are conserved. Therefore, a phase point can acquire two different values of the adiabatic invariant. The difference between the values corresponds to the area of the domain G_3 at the moment of separatrix crossing; i.e., it is approximately equal to the initial action. The question is how the initial bunch is divided, and what is the probability for a phase point to come into either of the two upper bunches? From the set of 100 points, 87 were trapped in the upper bunch, while 13 in the bottom. This numerical result is in very good accordance with the theoretical prediction for the probabilities (24) and (B5), which gives $\mathcal{P}_2=86.998$ (see Appendix B). In the case of nonzero AT considered in [24,25], the initial bunch would lie near the $w=-1$ line, and there would be only one "final" bunch. Here, there are separated bunches, which suggested us to introduce the terminology "separated AT."

Let $I=I(w,\theta,\tau)$, $\phi=\phi(w,\theta,\tau)$ mod 2π be the action-angle variables of the unperturbed (τ=const) problem. The "action" $I(w,\theta,\tau)$ multiplied by 2π is the area inside the unperturbed trajectory, passing through the point (w,θ) (provided the trajectory is closed; otherwise, the area of a domain bounded by the trajectory and lines $\theta=0,2\pi$ is calculated). The "angle" ϕ is a coordinate on the same unperturbed trajectory. It is measured from some curve transversal to the unperturbed trajectories. The change $(w,\theta)\to(I,\phi)$ is canonical (and can be done using a generating function which depends on τ). In the exact system (with $\dot{\tau}=\epsilon\neq 0$) the variables I and ϕ are canonically conjugated variables of the Hamiltonian

$$H = H_0(I,\tau) + \epsilon H_1(I,\phi,\tau), \tag{A1}$$

where $H_0(I,\tau)$ is the initial Hamiltonian $E(w,\theta,\tau)$ expressed in new variables, while the perturbation H_1 comes from the

time derivative of the generating function. In the case where the angle ϕ is measured from some straight line $\phi=$const, one has the formula [10]

$$H_1 = \frac{1}{\omega_0}\int_0^{\phi}\left(\frac{\partial E}{\partial \tau} - \left\langle \frac{\partial E}{\partial \tau}\right\rangle\right)d\phi, \quad \omega_0 = \frac{\partial H_0}{\partial I}, \tag{A2}$$

where the brackets $\langle\cdots\rangle$ denote averaging over the angle ϕ.

Consider a phase point of the exact system with the initial conditions $I=I_0$, $\phi=\phi_0$. The adiabatic approximation is obtained by omitting the last term in Eq. (A1) and gives

$$I = I_0, \quad \phi = \phi_0 + \frac{1}{\epsilon}\int_0^{\epsilon t}\omega_0(I,\tau)d\tau. \tag{A3}$$

The improved adiabatic approximation is introduced in the following way. One makes another canonical change of variables $(I,\phi)\to(J,\psi)$. The change is $O(\epsilon)$, close to the identity, and in the new variables the Hamiltonian has the form

$$H = H_0(J,\tau) + \epsilon\bar{H}_1(J,\tau) + \epsilon^2 H_2(J,\omega,\tau,\epsilon), \tag{A4}$$

$$\bar{H}_1 = \langle H_1\rangle = -\frac{1}{\omega_0}\int_0^{2\pi}\left(\frac{1}{2} - \frac{\phi}{2\pi}\right)\frac{\partial E}{\partial \tau}d\phi. \tag{A5}$$

The improved action variable can be defined as

$$J = J(w,\theta,\tau) + I + \epsilon u, \tag{A6}$$

$$u = u(w,\theta,\tau) = \frac{1}{2\pi}\int_0^{T}\left(\frac{T}{2} - t\right)\frac{\partial E}{\partial \tau}dt, \tag{A7}$$

where the integral is taken along the unperturbed trajectory passing the point (w,θ), $T=\frac{2\pi}{\omega_0}$ is the period of the trajectory, and the time t is measured starting from the point (w,θ). Determined in this way, $\langle u\rangle=0$. The improved adiabatic approximation is obtained by omitting the last term in Eq. (A5) and gives

$$J = J_0, \quad \psi = \psi_0 + \frac{1}{\epsilon}\int_0^{\epsilon t}[\omega_0(J,\tau) + \epsilon\omega_1(J,\tau)]d\tau,$$

$$\omega_1 = \frac{\partial \bar{F}_1}{\partial J}. \tag{A8}$$

APPENDIX B: PROBABILITIES OF CAPTURES DURING SEPARATED AT

We change both δ and λ linearly in time: $\delta=\delta_0-\epsilon t$, $\lambda=\lambda_0-\kappa\epsilon t$, $\kappa=1.5$; $\lambda_0=25$, $\delta_0=8$. We consider a bunch of $N=100$ trajectories with initial conditions $w_k=w_0+0.02\epsilon k$, $\theta_k=0$ ($w_0=-0.8$) which imply a distribution of initial actions in a tiny interval of order ϵ. Alternatively, one can consider initial conditions with the same initial action, but with the distribution along the angle variable ϕ. In any case, from N trajectories, approximately $\mathcal{P}_2N$ will be captured in domain G_2, and $\mathcal{P}_1N$ in domain G_1. As a result, after sweeping the value of δ to $-\infty$, one obtains two bunches of trajectories each closely distributed along two different values of action. This is a new phenomenon in the context of nonlinear Landau-Zener tunneling.

At the moment of separatrix crossing, the phase portrait looks like shown in Fig. 9(f). Phase flow from the domain G_3 is divided between G_1 and G_2. It is possible to calculate analytically the probabilities of captures in either domain. The separatrix crosses the line $\theta=0$ at points $w=w_{a,b}$, $w_a<w_b$ and the line $\theta=\pi$ at $w=w_s$ (the unstable fixed point). These three magnitudes $(w_{a,b,s})$ are roots of the equation

$$(\dot{w})^2 = 1 - w^2 - \left(h_s + \delta_* w - \frac{\lambda_*}{2}w^2\right)^2 = 0, \tag{B1}$$

where h_s is the energy on the separatrix at the moment of crossing and δ_* and λ_* are values of the parameters at this moment ($w=w_s$ is the doubly degenerate root). In other words,

$$\dot{w} = \pm\sqrt{-\frac{\lambda_*^2}{4}(w-w_a)(w-w_b)(w-w_s)^2}. \tag{B2}$$

The probabilities of capture in either domain are given by

$$\mathcal{P}_2 = \frac{I_2}{I_1}, \quad \mathcal{P}_1 = \frac{I_2 - I_1}{I_1},$$

$$I_{1,2} = \frac{1}{2}\oint_{l_{1,2}} dt\frac{\partial \bar{H}}{\partial \rho} = -\delta' I_{1,2}^{\delta} + \frac{\lambda'}{2}I_{1,2}^{\lambda} = -\delta'\int_{w_{a,b}}^{w_s} dw\frac{w-w_s}{\dot{w}} + \frac{\lambda'}{2}\int_{w_{a,b}}^{w_s} dw\frac{w^2-w_s^2}{\dot{w}}, \tag{B3}$$

where lower limits of integration for I_1, I_2 are w_a and w_b correspondingly. For value of $\dot{w}$ one uses the Eq. (B2) which makes the integrands in Eqs. (B3) simple, and one gets

$$\frac{\lambda}{2}I_1^{\delta} = \arcsin\left[\frac{-2w_s + w_a + w_b}{w_b - w_a}\right] - \pi/2,$$

$$\frac{\lambda}{2}I_1^{\lambda} = \sqrt{-(w_s-w_a)(w_s-w_b)} + (w_s + (w_a+w_b)/2)I_1^{\delta},$$

$$\frac{\lambda}{2}I_2^{\delta} = -\arcsin\left[\frac{-2w_s + w_a + w_b}{w_b - w_a}\right] - \pi/2,$$

$$\frac{\lambda}{2}I_2^{\lambda} = -\sqrt{-(w_s-w_a)(w_s-w_b)} + (w_s + (w_a+w_b)/2)I_2^{\delta}. \tag{B4}$$

Therefore,

$$\mathcal{P}_2 = \frac{I_2}{I_1} = \frac{-\delta'(-\alpha-\pi/2) + \frac{\lambda'}{2}[-Q_s + W_s(-\alpha-\pi/2)]}{-\delta'(\alpha-\pi/2) + \frac{\lambda'}{2}[Q_s + W_s(\alpha-\pi/2)]},$$

$$\alpha = \arcsin\left[\frac{-2w_s + w_a + w_b}{w_b - w_a}\right],$$

$$Q_s = \sqrt{-(w_s - w_a)(w_s - w_b)}, \quad W_s = w_s + (w_a + w_b)/2. \tag{B5}$$

In the numerical example presented in Fig. 11, $\delta' = -1$, $\lambda' = -\kappa = -1.5$; at the separatrix crossing, $\lambda_* = 8.386\,336\,9$, $\delta_* = -3.075\,775\,3$, $h_s = 0.355\,354\,4$. It gives $w_a \approx -0.923\,962\,8$, $w_b \approx 0.301\,551\,67$, $w_s \approx -0.422\,314\,9$. Formula (B5) gives $\mathcal{P}_2 \approx 86.998$, which perfectly corresponds to the numerical result (87%).

[1] P. Ehrenfest, Philos. Mag. **33**, 500 (1917); L. Navarro and E. Perez, Arch. Hist. Exact Sci. **60**, 209 (2006).
[2] A. Einstein, Sitzungsber. K. Preuss. Akad. Wiss. **3**, 18 (1925).
[3] F. London, Nature (London) **141**, 632 (1938).
[4] M. H. Anderson, J. R. Ensher, M. R. Matthews, C. E. Wieman, and E. A. Cornell, Science **269**, 198 (1995).
[5] K. B. Davis, M.-O. Mewes, M. R. Andrews, N. J. van Druten, D. S. Durfee, D. M. Kurn, and W. Ketterle, Phys. Rev. Lett. **75**, 3969 (1995).
[6] F. Dalfovo, S. Giorgini, L. P. Pitaevskii, and S. Stringari, Rev. Mod. Phys. **71**, 463 (1999); C. J. Pethick and H. Smith, *Bose-Einstein Condensation in Dilute Gases* (Cambridge University Press, Cambridge, England, 2001).
[7] L. P. Pitaevskii and S. Stringari, *Bose-Einstein Condensation* (Clarendon Press, Oxford, 2003)
[8] A. M. Dykhne, Sov. Phys. JETP **11**, 411 (1960).
[9] L. D. Landau and E. M. Lifshitz, *Quantum Mechanics* (Pergamon, Oxford, 1976).
[10] V. I. Arnold, V. V. Kozlov, and A. I. Neishtadt, *Mathematical aspects of classical and celestial mechanics*, Vol. 3 of *Encyclopedia of Mathematical Sciences*, 3rd ed. (Springer, Berlin, 2006).
[11] A. V. Timofeev, Sov. Phys. JETP **48**, 656 (1978).
[12] J. R. Cary, D. F. Escande, and J. L. Tennyson, Phys. Rev. A **34**, 4256 (1986).
[13] A. I. Neishtadt, Sov. J. Plasma Phys. **12**, 568 (1986).
[14] A. I. Neishtadt, PMM U.S.S.R. **51**, 586 (1987).
[15] J. R. Cary and R. T. Skodje, Physica D **36**, 287 (1989); D. L. Bruhwiler and J. R. Cary, *ibid.* **40**, 265 (1989); R. T. Skodje, J. Chem. Phys. **95**, 7234 (1991).
[16] A. P. Itin, A. I. Neishtadt, and A. A. Vasiliev, Physica D **141**, 281 (2000).
[17] A. I. Neishtadt and A. A. Vasiliev, Nonlinearity **12**, 303 (1999); D. L. Vainshtein, A. A. Vasiliev, and A. I. Neishtadt, Chaos **6**, 67 (1996).
[18] A. P. Itin, A. A. Vasiliev, and A. I. Neishtadt, J. Math. Sci. (N.Y.) **128**, 2778 (2005); also available in Russian: Zap. Nauchn. Semin. POMI **300**, 173 (2003).
[19] A. P. Itin, A. I. Neishtadt, and A. A. Vasiliev, Phys. Lett. A **291**, 133 (2001); A. P. Itin and A. I. Neishtadt, Regular Chaotic Dyn. **8**, 59 (2003); A. P. Itin, Plasma Phys. Rep. **28**, 592 (2002); Phys. Lett. A **324**, 159 (2004); Phys. Rev. E **67**, 026601 (2003).
[20] A. P. Itin, R. de la Llave, A. I. Neishtadt, and A. A. Vasiliev, Chaos **12**, 1043 (2002).
[21] K. Dietz, J. Henkel, and M. Holthaus, Phys. Rev. A **45**, 4960 (1992).
[22] *Chaotic Dynamics and Transport in Quantum and Classical Systems*, edited by P. Collet, M. Courbage, S. Metens, G. M. Zaslavsky, and A. I. Neishtadt (Kluwer, Dordrecht, 2004); G. M. Zaslavsky, *Physics of Chaos in Hamiltonian Dynamics* (Imperial College Press, London, 1998).
[23] A. Smerzi, S. Fantoni, S. Giovanazzi, and S. R. Shenoy, Phys. Rev. Lett. **79**, 4950 (1997).
[24] O. Zobay and B. M. Garraway, Phys. Rev. A **61**, 033603 (2000).
[25] J. Liu, L. Fu, B. Ou, S. Chen, D. Choi, B. Wu, and Q. Niu, Phys. Rev. A **66**, 023404 (2002).
[26] E. Pazy, I. Tikhonenkov, Y. B. Band, M. Fleischhaner, and A. Vardi, Phys. Rev. Lett. **95**, 170403 (2005); I. Tikhonenkov, E. Pazy, Y. B. Band, M. Fleischhaner, and A. Vardi, Phys. Rev. A **73**, 043605 (2006).
[27] A. P. Itin, A. A. Vasiliev, and S. Watanabe (unpublished).
[28] A. P. Itin *et al.* (unpublished) (see also http://power1.pc.uec.ac.jp/~alx_it); A. P. Itin, A. A. Vasiliev, G. Krishna, and S. Wantanabe, Physica D **232**, 108 (2007).
[29] Z. P. Karkuszewski, K. Sacha, and J. Zakrzewski, Phys. Rev. A **63**, 061601(R) (2001).
[30] F. Kh. Abdullaev and R. A. Kraenkel, Phys. Rev. A **62**, 023613 (2000).
[31] P. V. Elyutin and A. N. Rogovenko, Phys. Rev. E **63**, 026610 (2001).
[32] E. A. Ostrovskaya, Yu. S. Kivshar, M. Lisak, B. Hall, F. Cattani, and D. Anderson, Phys. Rev. A **61**, 031601(R) (2000).
[33] K. W. Mahmud, H. Perry, and W. P. Reinhardt, Phys. Rev. A **71**, 023615 (2005).
[34] T. Miyakawa and P. Meystre, Phys. Rev. A **71**, 033624 (2005).
[35] A. Vardi, V. A. Yurovsky, and J. R. Anglin, Phys. Rev. A **64**, 063611 (2001).
[36] G. J. Milburn, J. Corney, E. M. Wright, and D. F. Walls, Phys. Rev. A **55**, 4318 (1997); G. L. Salmond, C. A. Holmes, and G. J. Milburn, *ibid.* **65**, 033623 (2002); A. P. Hines, R. H. McKenzie, and G. J. Milburn, *ibid.* **67**, 013609 (2003).
[37] S. K. Adhikari, Phys. Rev. E **63**, 056704 (2001).
[38] D. Ananikian and T. Bergeman, Phys. Rev. A **73**, 013604 (2006).
[39] J. Javanainen, M. Kostrun, Y. Zheng, A. Carmichael, U. Shrestha, P. Meinel, M. Mackie, O. Dannenberg, and K. A. Suominen, Phys. Rev. Lett. **92**, 200402 (2004).
[40] J. Javanainen and M. Mackie, Phys. Rev. A **59**, R3186 (1999).
[41] E. Timmermans, P. Tommasini, R. Cote, M. Hussein, and A. Kerman, Phys. Rev. Lett. **83**, 2691 (1999); Phys. Rep. **315**, 199 (1999).
[42] R. A. Barankov and L. S. Levitov, Phys. Rev. Lett. **93**, 130403 (2004); A. V. Andreev, V. Gurarie, and L. Radzihovsky, Phys. Rev. Lett. **93**, 130402 (2004); J. Dukelsky, G. G. Dussel, C. Esebbag, and S. Pittel, Phys. Rev. Lett. **93**, 050403 (2004).
[43] G. Santos, A. Tonel, A. Foerster, and J. Links, Phys. Rev. A

73, 023609 (2006).
[44] E. A. Yuzbashyan, B. L. Altshuler, V. B. Kuznetsov, and V. Z. Enolskii, J. Phys. A **38**, 7831 (2005).
[45] I. M. Lifshitz, A. A. Slutskin, and V. M. Nabutovskii, Sov. Phys. JETP **14**, 669 (1962).
[46] A. I. Neishtadt, Prikl. Mat. Mekh. **39**, 1331 (1975).
[47] A. A. Vasiliev, A. P. Itin, and A. I. Neishtadt, Regular Chaotic Dyn. **2**, 21 (1997).
[48] V. I. Arnold, Russ. Math. Surveys **18**, 85 (1963).
[49] Note that the geometric change in the action is accompanied by the nontrivial ϵ-dependent *dynamical* change mentioned above. It is usually the *dynamical* change in the action which causes the *destruction* of *adiabatic invariance*.
[50] M. K. Oberthaler (private communication).
[51] M. Albiez, R. Gati, J. Folling, S. Hunsmann, M. Cristiani, and M. K. Oberthaler, Phys. Rev. Lett. **95**, 010402 (2005).
[52] A. Ishkhanyan *et al.*, in *Interactions in Ultracold Gases: From Atoms to Molecules*, edited by M. Weidemuller and K. Zimmermann (Wiley-Vch, Berlin, 2003); M. Mackie *et al.*, *ibid*.
[53] T. Koehler, K. Goral, and P. S. Julienne, Rev. Mod. Phys. **78**, 1311 (2006).
[54] C. A. Regal *et al.*, Nature (London) **424**, 47 (2003).
[55] K. E. Strecker, G. B. Partridge, and R. G. Hulet, Phys. Rev. Lett. **91**, 080406 (2003).
[56] J. Cubizolles, T. Bourdel, S. J. J. M. F. Kokkelmans, G. V. Shlyapnikov, and C. Salomon, Phys. Rev. Lett. **91**, 240401 (2003).
[57] E. Hodby, S. T. Thompson, C. A. Regal, M. Greiner, A. C. Wilson, D. S. Jin, E. A. Cornell, and C. E. Wieman, Phys. Rev. Lett. **94**, 120402 (2005).
[58] A. E. Leanhardt, A. Gorlitz, A. P. Chikkatur, D. Kielpinski, Y. Shin, D. E. Pritchard, and W. Ketterle, Phys. Rev. Lett. **89**, 190403 (2002); Y. Kawaguchi, M. Nakahara, and T. Ohmi, Phys. Rev. A **70**, 043605 (2004); Y. Shin, C. Sanner, G. B. Jo, T. A. Pasquini, M. Saba, W. Ketterle, D. E. Pritchard, M. Vengalattore, and M. Prentiss, *ibid.* **72**, 021604(R) (2005); A. P. Itin, T. Morishita, M. Satoh, O. I. Tolstikhin, and S. Watanabe, *ibid.* **73**, 063615 (2006).
[59] H. Saito and M. Ueda, Phys. Rev. Lett. **90**, 040403 (2003); F. K. Abdullaev, J. G. Caputo, R. A. Kraenkel, and B. A. Malomed, Phys. Rev. A **67**, 013605 (2003); A. P. Itin, T. Morishita, and S. Watanabe, *ibid.* **74**, 033613 (2006).
[60] R. Kanamoto, H. Saito, and M. Ueda, Phys. Rev. Lett. **94**, 090404 (2005); A. P. Itin and S. Watanabe (unpublished).
[61] D. Witthaut, E. M. Graefe, and H. J. Korsch, Phys. Rev. A **73**, 063609 (2006); E. M. Graefe and H. J. Korsch, arXiv: quant-ph/611010 (unpublished).
[62] M. Holthaus and S. Stenholm, Eur. Phys. J. B **20**, 451 (2001).